Journal of Hazardous Materials 166 (2009) 714–719

Contents lists available at ScienceDirect

Journal of Hazardous Materials

journal homepage: www.elsevier.com/locate/jhazmat

Preparation of a new sorbent with hydrated lime and blast furnace slag for phosphorus removal from aqueous solution

Guozhuo Gong[a,b], Shufeng Ye[a,*], Yajun Tian[a], Qi Wang[c], Jiandi Ni[a,b], Yunfa Chen[a]

[a] State Key Laboratory of Multi-phase Complex System, Institute of Process Engineering, Chinese Academy of Sciences, Beijing 100080, PR China
[b] Graduate University of Chinese Academy of Sciences, Beijing 100049, PR China
[c] School of Metallurgical Engineering, Xi'An University of Architecture and Technology, Xi'An 710055, PR China

ARTICLE INFO

Article history:
Received 17 March 2008
Received in revised form
25 November 2008
Accepted 25 November 2008
Available online 30 November 2008

Keywords:
Phosphate removal
Blast furnace slag
Hydrated lime

ABSTRACT

The removal of dissolvable inorganic phosphate ($H_2PO_4^-$) by sorbents prepared from hydrated lime (HL) and blast furnace slag (BFS) was fundamentally studied by an orthogonal experiment design. Based on statistic analysis, it is revealed that the weight ratio of BFS/HL is the most significant variable, and an optimized preparation condition is figured out. With the increase of HL content, the adsorption capacity increases, suggesting that the HL plays the important role in the removal process in the gross. However, in the lower HL content, it is interesting that the adsorption capacity of as-prepared sorbents exceed the sum of the capacities of the same ratio of BFS and HL. The further analysis indicate the excess capacities linearly depend on the specific surface area of sorbents, suggesting that the removal of $H_2PO_4^-$ is closely related with the microstructure of sorbents in the lower HL content, according to the characterization with SEM, XRD and pore analysis. Additionally, an adsorption model and kinetic are discussed in this paper.

1. Introduction

Phosphorus (P) exists in many consumer products and industrial processes involving particles of a colloidal nature. Examples of such applications are as diverse as fertilizers, detergents, pigment formulation, water treatment and mineral processing. P discharged into the surface waters stimulates the growth of aquatic micro- and macro-organisms in nuisance quantities, which in excess can cause eutrophication in stagnant water bodies [1–5]. Therefore, removal of P from the wastewater is necessary for the control of eutrophication in lakes and similar stagnant water bodies [6,7].

Many methods have been developed to remove excessive P from water [8–22]. Biological method is a low-cost one, but the fluctuation in chemical composition and temperature of wastewater makes the process running unfeasible [12,22]. The techniques such as adsorption, chemical precipitation are more economical than ion exchange and electrodialysis [13,22], and have been employed in industry. Nevertheless, to find the cheap and effective sorbent is still highly desired, although various sorbents including activated aluminium oxide [8], fly ash [10–13], zeolite [17,18], different soils [9,12,15,18] and activated carbon [21,22] have been investigated.

Blast furnace slag (BFS) is a waste discharged from steel factory in large scale, and the environment impact caused by BFS is becoming evident more and more, thus how to utilize or reuse BFS is a significant issue. Recently, some attempts have been carried to apply BFS into a sorbent to remove the dissolvable P from aqueous solution [1,4,5,11,14,16,19,22], and the removal mechanisms of P by BFS were discussed. It was expected the calcium-based substances contained in BFS is the active components for dissolvable P, and it also was pointed that the removal of P is related with other elements including Al, Mg, Fe, Mn and Ti exposed on the surface of BFS, besides Ca [1]. Oguz [22] suggested that the removal of phosphate by BFS predominantly took place by precipitation mechanism, ion exchange and weak physical interactions between the surface of sorbent and the metallic salts of phosphate. However, the application of slag in the adsorption of P from aqueous solutions faces a number of problems, too [4]. BFS is a complex system of $CaO–MgO–Al_2O_3–SiO_2$ which also incorporates a number of minor components that can concentrate on the slag surface during crystallization or during transition to the glassy state, and can affect the adsorption of phosphates. Furthermore, because of its low specific surface area and poor pore structure, the internal chemical components cannot be used efficiently. Therefore, how to activate the BFS surface is one of the effective ways to utilize this waste.

In this article, hydrated lime (HL) was used as an activator to modify the surface of BFS to improve the P adsorption capacity. A series of BFS–HL sorbents for phosphate removal were prepared

* Corresponding author. Tel.: +86 10 62588029; fax: +86 10 62542803.
E-mail addresses: gzgong@home.ipe.ac.cn (G. Gong), sfye@home.ipe.ac.cn (S. Ye).

0304-3894/$ – see front matter © 2008 Elsevier B.V. All rights reserved.
doi:10.1016/j.jhazmat.2008.11.077

Table 1
Chemical composition and physical properties of $Ca(OH)_2$ and BFS.

Chemical composition (wt%)	BFS	$Ca(OH)_2$
SiO_2	33.26	
Al_2O_3	15.63	
FeO	0.83	<0.01
MgO	9.41	<0.5
CaO	38.69	
SO_3	0.35	
$Ca(OH)_2$		>95
$CaCO_3$		<2
Insoluble		<0.05
Ignition loss	0.52	
Physical properties		
Particle mean diameter (μm)	4.3	7.9
BET specific surface area ($m^2\,g^{-1}$)	17.95	8.70
True density ($g\,cm^{-3}$)	2.30	2.13

based on an orthogonal experiment design. The ratio of BFS to HL was found to be the most significant factor to the absorption capacity of P, and the relationship between the absorption capacity and microstructure of sorbents was discussed in combination of the characterizations. The equilibrium model and absorption kinetic were also studied.

2. Materials and methods

2.1. Sorbents preparation and designs of experiment

Sorbents were prepared using commercial $Ca(OH)_2$ (supplied by Beijing Chemical Reagents Company) and BFS (supplied by Jinan Iron and Steel Company Limited of China). Their chemical composition and physical properties are shown in Table 1.

A full factorial design was used to synthesize sorbents by varying four experimental variables: the hydration time (t_s), weight ratio of blast furnace slag to hydrated lime (BFS/HL), the slurrying temperature (T) and the ratio of water to solid (W/S). Total mass of $Ca(OH)_2$ plus BFS was kept at a constant value of 15 g for all the samples. Table 2 displays the matrix of the L_{16} (4^4) factorial design. The procedure used to prepare the sorbents comprised the following steps. BFS–HL slurry was added at the required ratio in a 250 ml polypropylene conical beaker that was heated by an electric thermostatic oil bath pan equipped with a magnetic stirrer at a constant rate of 700 rpm. The mouth of the beaker was plugged to prevent water loss and the interference of CO_2. After slurrying the sample was placed into a vacuum oven at 35 °C for about 24 h to evaporate most of the free water and then further heated to 120 °C to dry, which was in about 2–4 days. The dried sorbents were then pelletized, crushed and sieved to produce the required particle size range (60–100 μm).

2.2. Adsorption experiment

2.2.1. Batch experiment

Phosphorus removal tests of BFS–HL sorbents, $Ca(OH)_2$ and BFS were conducted through batch experiments. 0.2 g of sorbent was added into a 250 ml conical flask containing 100 ml KH_2PO_4 (as P) solution with concentration of 200 mg L^{-1}, and then shaken by a horizontal bench shaker for 6 h (the time required for equilibrium to be reached between phosphorus adsorbed and phosphorus in solution for all BFS–HL sorbents) using a bath at temperature at 30 ± 1 °C. The pH of solution was measured with pH meter (Lei Ci made in Shanghai) after the adsorption without buffer or controlled. At the end of the adsorption period, the samples were filtrated by filter paper and the clear filtrates were taken and analyzed for phosphate. The amount of phosphate adsorbed per unit of sorbents was calculated by

$$q = \frac{(c_i - c_e)V}{m} \quad (1)$$

where q (mg g^{-1}) is the amount of the phosphate adsorbed per unit mass of sorbent (adsorption capacity), c_i (mg L^{-1}) and c_e (mg L^{-1}) are the initial and final concentrations of the phosphate in solution, respectively, V (L) is the solution volume, and m (g) is the mass of sorbent used. The phosphate concentration in solution was measured by a spectrophotometer (721 made in Shanghai).

2.2.2. Kinetics and equilibrium study

Adsorption kinetics experiment was carried out using 100 ml of KH_2PO_4 solution with the desired concentration and 0.2 g sorbent in a 250 ml conical flasks shaking by water shaker. At predetermined time intervals, samples were separated by filter paper and analyzed by spectrophotometer. Adsorption isotherms experiment was very similar with adsorption kinetics, the difference was that adsorption isotherms were carried out with different initial KH_2PO_4 concentrations and the pH values of solutions were adjusted to 7 by HCl or NaOH solution prior to adsorption.

2.3. Characterization of sorbents

Scanning electron microscopy (SEM) photographs of the sorbents were taken in a JEOL, JSM-6700F system, in order to learn

Table 2
Experimental design and results of BFS–HL sorbents and raw materials.

Solid code	Preparation variables				Results			
	t_s (h)	W/S (g g^{-1})	BFS/HL (g g^{-1})	T (°C)	q (mg g^{-1})	$Incr_s$ (mg g^{-1})	S_{BET} ($m^2\,g^{-1}$)	pH value
S1	0.75	10/1	9/1	50	84.70	39.62	37.80	7.08
S2	0.75	15/1	7/3	60	114.15	29.15	27.00	7.52
S3	0.75	20/1	3/7	70	165.08	0.72	24.36	8.92
S4	0.75	25/1	1/9	80	203.97	−0.15	14.53	11.29
S5	4	10/1	7/3	70	118.23	33.15	29.08	7.48
S6	4	15/1	9/1	80	87.18	42.10	45.84	7.19
S7	4	20/1	1/9	50	202.97	−1.15	26.45	11.21
S8	4	25/1	3/7	60	166.06	1.64	42.51	10.37
S9	10	10/1	3/7	80	163.84	−0.52	29.09	9.11
S10	10	15/1	1/9	70	203.54	−1.12	17.49	11.5
S11	10	20/1	9/1	60	103.26	57.91	62.39	7.26
S12	10	25/1	7/3	50	120.15	35.15	40.03	7.21
S13	17	10/1	1/9	60	204.80	0.68	19.20	11.24
S14	17	15/1	3/7	50	165.08	0.72	32.47	8.46
S15	17	20/1	7/3	80	120.29	35.15	36.92	7.57
S16	17	25/1	9/1	70	99.58	54.49	60.12	7.17
$Ca(OH)_2$	–	–	–	–	224.18	–	8.70	11.67
BFS	–	–	–	–	25.21	–	17.95	6.81

Table 3
Results of the ANOVA test for P adsorption capacity of BFS–HL sorbents.

Factors	Sum of squares	d.f.[a]	Mean square	*F*-ratio	*P*[b]
t_s	98.81	3	32.94	3.02	0.19
W/S	96.50	3	32.17	2.95	0.20
BFS/HL	28739.98	3	9579.99	878.09	6E−05
T	45.29	3	15.10	1.38	0.40
Total error	32.73	3	10.91		

[a] Degrees of freedom.
[b] Probability for *F*-ratio test.

the change of microstructure caused by hydration reaction. X-ray diffraction (XRD) patterns were recorded by a Panalytical X'Pert PRO system with the powdered samples less than 100 μm, with Cu Kα radiation in the diffraction angle (2θ) range of 5–70° at a sweep rate of 3° min^{-1}. Nitrogen adsorption isotherms were obtained at 77K with the aid of a conventional volumetric apparatus (Autosorb-1-MP). The equivalent surface area was obtained from the linear BET plots (S_{BET}), and the pore size distribution of samples was calculated by BJH method.

3. Results and discussion

3.1. Effect of preparation variables on the P adsorption

The results of P adsorption capacity for the BFS–HL sorbents prepared under various conditions and raw materials of $Ca(OH)_2$ and BFS are listed in Table 2. It is clear that all BFS–HL sorbents show lower P adsorption capacity than $Ca(OH)_2$, but much higher than BFS.

A statistical method is used based on analysis of the variance (ANOVA) which determines the statistical signification of factors by comparing their mean squares with an estimation of experimental error.

In Table 3, the weight ratio of BFS/HL has *P*-value less than 0.001, indicating that it is significantly different from zero at the 99.9% confidence level, and is the most important variable for P adsorption. The hydration time (45 min to 17 h), the ratio of water/solid (10/1 to 25/1) and the slurrying temperature (50–80 °C) have *P*-values more than 0.1, indicating that their influences on P adsorption are weak. So it is concluded that the reaction of BFS with HL almost complete within 45 min, and when the slurrying time is longer than 45 min, the increase of P adsorption capacity of BFS–HL sorbent is less profound. The ratio of water/solid can be controlled to 10/1, and within the range of 50–80 °C, it is not necessary to control the temperature accurately especially in the industry application.

Fig. 1 shows the relationship of P adsorption capacity with the weight ratio of BFS in the preparation procedure of sorbent. It can be found that with the decrease of the weight ratio of BFS, P adsorption capacity of sorbent increases rapidly. This is well understood since the P adsorption capacity of $Ca(OH)_2$ is high.

3.2. Effect of modification method on the P adsorption of sorbent

To understand the effect of modification on the P adsorption, the difference between the P adsorption capacity of sorbent and those of the same ratio of raw materials is calculated according to the following equation:

$$Incr_s = q_s - W_{BFS}q_{BFS} - (1 - W_{BFS})q_{HL} \quad (2)$$

where $Incr_s$ is the increment of P adsorption capacity for sorbent, q_s is the P adsorption capacity for sorbent, W_{BFS} is the weight ratio of BFS in the preparation procedure of sorbent, q_{BFS} is the P adsorption capacity of BFS, and q_{HL} is the P adsorption capacity

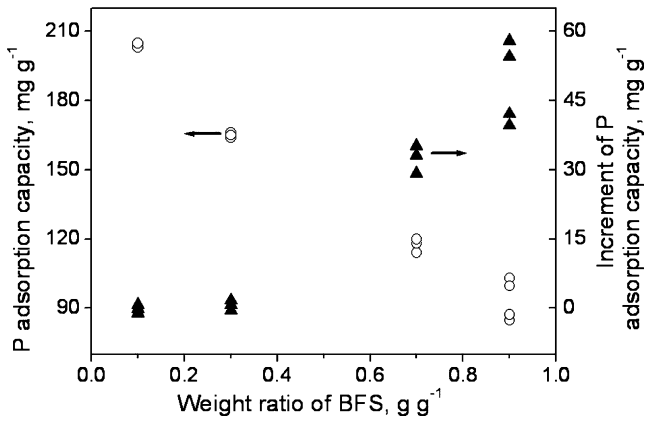

Fig. 1. P adsorption capacity and the increment as a function of the weight raito of BFS for BFS–HL sorbents.

Table 4
Results of the ANOVA test for $Incr_s$ of sorbents.

Factors	Sum of squares	d.f.[a]	Mean square	*F*-ratio	*P*[b]
t_s	92.52	3	30.84	2.48	0.24
W/S	100.78	3	33.59	2.70	0.22
BFS/HL	7114.40	3	2371.47	190.94	6E−4
T	42.52	3	14.17	1.14	0.46
Total error	37.26	3	12.42		

[a] Degrees of freedom.
[b] Probability for *F*-ratio test.

of $Ca(OH)_2$. Table 2 shows the results of $Incr_s$ for all BFS–HL sorbents. The ANOVA analysis indicates the weight ratio of BFS/HL is the most significant factor for $Incr_s$, and the effects of other preparation variables are negligible (Table 4), which is consistent with the P absorption capacity.

The relationship of $Incr_s$ with the weight ratio of BFS is shown in Fig. 1. It can be found that with the increase of the weight ratio of BFS, $Incr_s$ increases rapidly, and when the weight ratio of BFS is 0.9, $Incr_s$ is the biggest.

3.3. Characterization of sorbents

Fig. 2 shows the pore size distribution of S16 and BFS measured by N_2 adsorption/desorption isotherm. It is found that S16 has the richer porosity than BFS, revealing the function of HL. Compared to BFS, the pore of BFS–HL sorbent shifts toward larger size, which is helpful for removal of P from aqueous solutions [3].

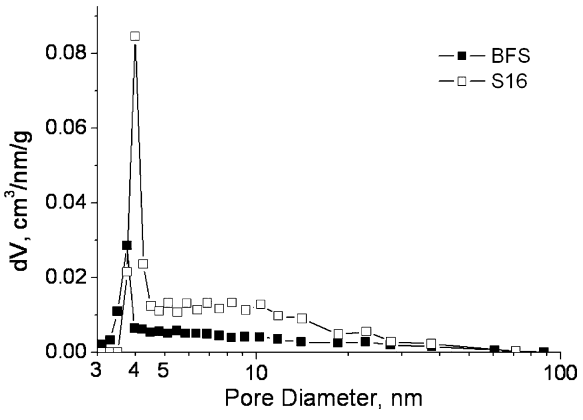

Fig. 2. Pore size distribution of S16 and BFS.

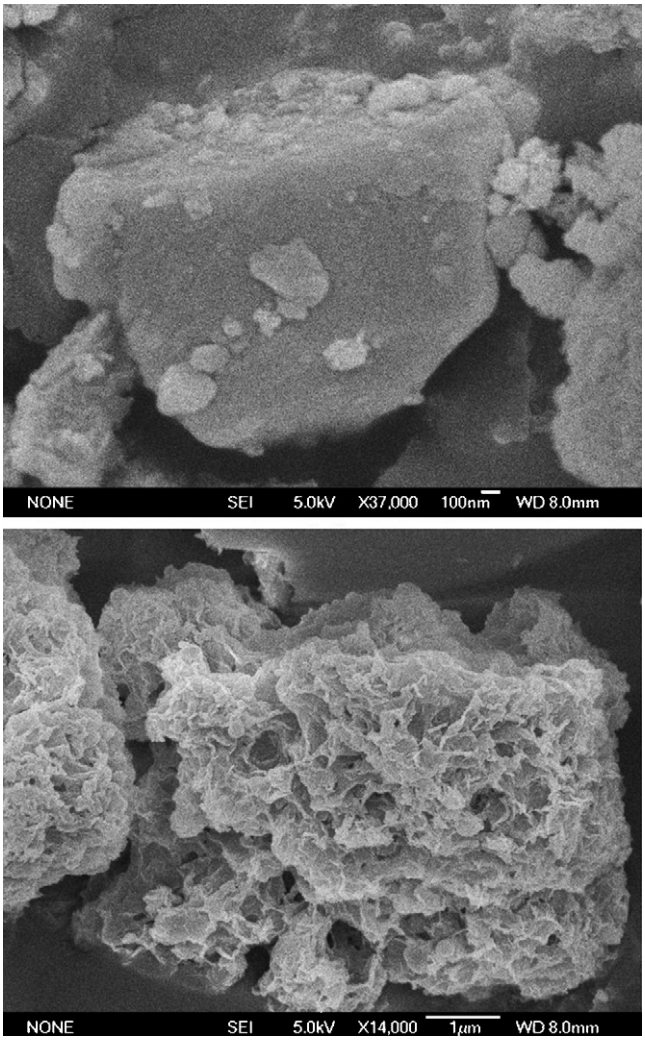

Fig. 3. SEM photographs of (a) BFS and (b) S16.

Table 2 summarizes the specific surface areas of sorbents. It was found that nearly all of the BFS–HL sorbents have larger surface areas than their raw materials of HL and BFS, probably due to pozzolanic reactions [23]. In general, pozzolanic reactions start with the chemical adsorption of calcium hydroxide on the surface of silanol groups [24]. Since the pH of the solution is high, SiO_2 is dissolved, reacting with $Ca(OH)_2$ to form calcium silicate (CSHs) which has large surface area and porous structure as follows:

$$SiO_2(s) + xCa^{2+}_{aq} + 2xOH^{-}_{aq} + (y-x)H_2O \rightarrow xCaO \cdot SiO_2 \cdot yH_2O \quad (3)$$

where x is 0.8–1.5, and y is 0.5–2.5 [25].

The SEM images of BFS and S16 are shown in Fig. 3. Fig. 3(a) is the typical morphology of a BFS particle discharged from a steel factory. Coarse surface and irregular shape of the particle is readily apparent. Fig. 3(b) shows the typical view of sorbent S16 which is very different from that of BFS. The surface of BFS particle is destroyed, more surface emerges and some "foil-like" material covers on the surface of the slag particle, which can also be found in other BFS–HL sorbents.

The XRD patterns of BFS and S16 are shown in Fig. 4. Obviously, the irregular diffraction pattern of BFS means it is amorphous. The XRD pattern of S16 shows the existence of $Ca(OH)_2$ and CSHs which can be seen in other sorbents. Compared with $Ca(OH)_2$, the peaks of calcium silicate (CSHs) are weaker and belong to illcrystallized tobermorites (2θ = 29.0–29.8°, 32°, and 49.8°). Illcrystallized

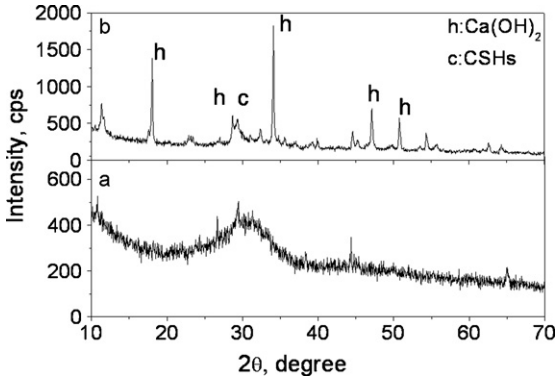

Fig. 4. X-ray patterns of the powdered sample: (a) BFS and (b) S16.

tobermorited include C–S–H(I), C–S–H(II), and tobermorite gel [25]. Under our experimental conditions, C–S–H(I) is the major product, which is similar with the CSHs phase formed in the HL–silica sorbents prepared by other researchers [26,27].

Fig. 5 illustrates the relationship betweent $Incr_s$ and the specific surface area of sorbents. When the weight ratio of BFS/HL is between 7/3 and 9/1, $Incr_s$ is seen to increase linearly from 29.15 to 57.91 mg g^{-1} as the specific surface area increases from 27.00 to 62.39 m^2 g^{-1}. This is a strong hint that the excess P adsorption capacity is attributed to the generation of pore structures over the BFS particles.

In the higher weight ratio of BFS/HL, the pH value of the absorption system is between 7 and 8. In this range of pH value, phosphate removal probably occurs with ion exchange mechanisms of phosphate hydrolysis products ($H_2PO_4^-$ and HPO_4^{2-}) and the precipitation of the metallic salts of phosphate (Al^{3+}, Ca^{2+} and Fe^{3+}) [22]. In this case, sorbent which has improved specific surface area can provide more ions to remove P and its P adsorption capacity is improved accordingly.

When the weight ratio of BFS/HL is between 1/9 and 3/7, the increment of P adsorption capacity is closed to zero and the influence of pozzolanic reactions seem disappear certainly. In this range of the weight ratio of BFS/HL, pH value in the solution was larger than 8.5. In this range of pH value, it is thought that phosphate removal took place by precipitation mechanism and the weak physical interactions between the surface of adsorbent and the metallic salts of phosphate [22]. Moreover, from Fig. 1, it can be seen that there are larger amount of reaction products in lower weight ratio of BFS/HL than that in higher weight ratio of BFS/HL. In this case, the precipitations of $AlPO_4$, $FePO_4$ and $Ca_3(PO_4)_2$ occurred on the sorbent surface [5,22], and the pore in the sorbent was probably

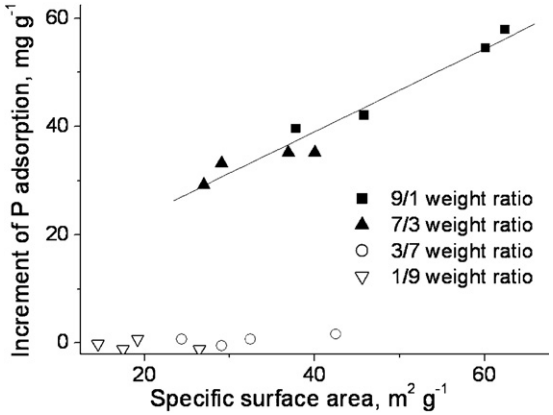

Fig. 5. Relationship between specific surface area and mesopore volume for BFS–HL sorbents.

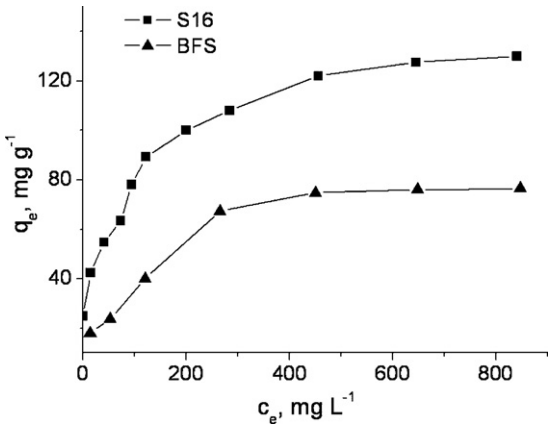

Fig. 6. Adsorption isotherms of P by BFS and S16.

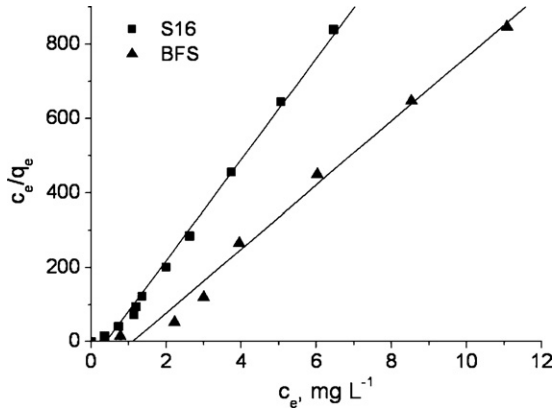

Fig. 7. The linearized Langmuir isotherm of P adsorption by BFS and S16.

blocked by the large amount of reaction products during the reaction process. As a result the contribution of the fresh surface or porosity structure disappeared.

3.4. Equilibrium studies

Adsorption isotherms are important for the description of how molecules of adsorbate interact with sorbent surface. Hence, the correlation of equilibrium data using either a theoretical or empirical equation is essential for the adsorption interpretation and prediction of the extent of adsorption. Two well-known isotherm equations, Langmuir model and Freundlich model, were tried for deeper interpretation of the adsorption data obtained. Fig. 6 shows the adsorption isotherms of BFS and S16. It is found that the saturated adsorption capacity of S16 is higher than that of BFS.

The Langmuir model with linear form is represented by Eq. (4) [6]:

$$\frac{c_e}{q_e} = \frac{1}{q_m K_a} + \frac{c_e}{q_m} \tag{4}$$

where q_e (mg g^{-1}) is the amount of solute adsorbed per gram of sorbent and c_e (mg L^{-1}) is the equilibrium concentration of solute in the bulk of the solution. The constants K_a (L mg^{-1}) and q_m (mg g^{-1}) relate to the ion-exchange capacity and energy of ion-exchange, respectively.

The Freundlich equation is given as linear form by Eq. (5) [6]:

$$\log q_e = \frac{1}{n \log c_e + \log K_f} \tag{5}$$

where K_f (mg g^{-1}) and n (g L^{-1}) are constants which relate to adsorption capacity and adsorption intensity of sorbent.

The values of the parameters of the two models and the related correlation coefficients (R^2 values) are listed in Table 5. The results show that the Langmuir equation better fits the adsorption equilibrium data over the concentration range used in this investigation than the Freundlich equation does. The linearized Langmuir isotherm of P adsorption by BFS and S16 are shown in Fig. 7. The reason that the Langmuir isotherm more fits the experimental data probably due to the homogeneous distribution of active sites on the surface of sorbent, in accordance with the Langmuir equation assumes that the surface is homogeneous and that the active sites have equal affinities for the molecules of the adsorbate.

Table 5
Langmuir and Freundlich isotherms parameters at 303 K.

Sorbent	Langmuir			Freundlich		
	q_m (mg g^{-1})	K_a (L mg^{-1})	R^2	K_f (mg g^{-1})	$1/n$ (L g^{-1})	R^2
S16	135.14	0.0031	0.9993	25.86	0.23	0.9055
BFS	86.96	0.0037	0.9886	5.893	0.40	0.9505

3.5. Kinetic studies

In order to obtain kinetic data for phosphate adsorption on BFS–HL sorbent, the variation in phosphate concentration with time was measured. The experimental results are presented in Fig. 8. It is found that the adsorption of P has an increasing trend along with time. Compared to BFS, adsorption of P for S16 is quicker and greater in the first hour, which is helpful for technical application. Furthermore, S16 is quicker than BFS to reach equilibrium.

Although many mathematical models such as homogeneous diffusion model and pore diffusion model have been proposed to interpret the transport of solutes inside adsorbents, the mathematical complexity of the models makes them inconvenient in practice [28]. The pseudo-first-order (Eq. (6)) and pseudo-second-order (Eq. (7)) kinetic models were selected to test the ion-exchange dynamics in this work because of their good applicability in many cases [6]:

$$\log\ (q_e - q_t) = \log q_e - k_1 t \tag{6}$$

$$\frac{t}{q_t} = \frac{1}{k_2 q_e{}^2} + \left(\frac{1}{q_e}\right) t \tag{7}$$

where q_t (mg g^{-1}) is the amount of P adsorption capacity at the time t (min), and k_1 (min^{-1}) and k_2 (g mg^{-1} min^{-1}) are the rate constants of the pseudo-first- and pseudo-second-order kinetic equations. The slopes and intercepts of these curves are used to determine the constants k_1 and k_2 and the equilibrium capacity q_e. The calculated (cal) value of q_e (Table 6) from the pseudo-first-order kinetics model

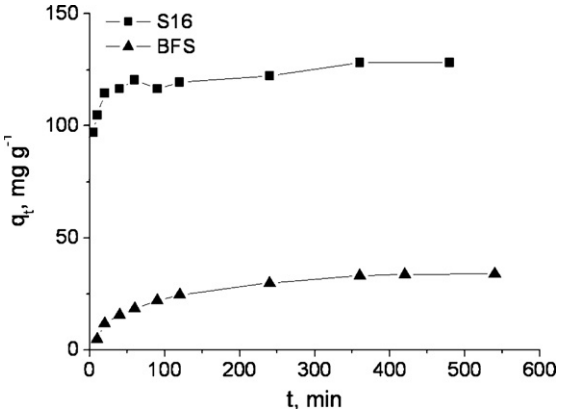

Fig. 8. Effect of contact time on P adsorption by BFS and S16.

Table 6
Kinetic constants for P adsorption by BFS and S16.

Sorbent	q_e(exp) (mg g^{-1})	Pseudo-first-order kinetics			Pseudo-second-order kinetics		
		q_e(cal) (mg g^{-1})	k_1 (min^{-1})	R^2	q_e(cal) (mg g^{-1})	k_2 (g mg^{-1} min^{-1})	R^2
S16	128.16	18.59	0.0024	0.6302	128.21	0.0016	0.9994
BFS	39.20	33.87	0.0051	0.9564	38.17	0.0004	0.9983

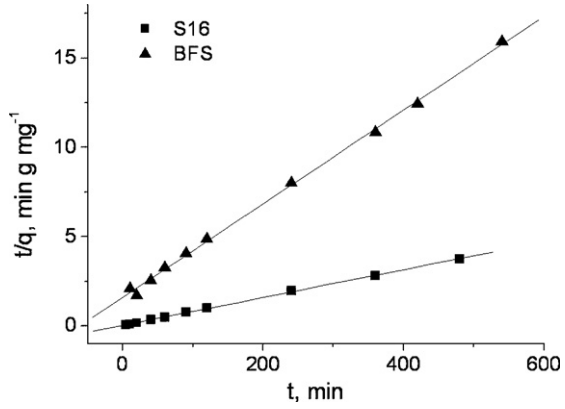

Fig. 9. The linearized pseudo-second-order kinetics plots for P adsorption by BFS and S16.

is dramatically lower than the experimental (exp) value. However, the pseudo-second-order kinetics model (Fig. 9, Table 6) provides a near-perfect match between the theoretical and experimental q_e values, and the pseudo-second-order equation has a better correlation with the experimental data than the pseudo-first-order equation. As a result, the process appears to follow pseudo-second-order reaction kinetics, which suggests that the use of this model approach can be a reliable tool when predicting phosphate adsorption in systems with contact times.

4. Conclusions

BFS–HL sorbent was successfully prepared and applied into P adsorption from $H_2PO_4^-$ solution. The results showed that the modification of BFS surface by HL can generate more pore structure, the inner chemical material in BFS could be used and the P adsorption capacity of BFS was improved by this mechanism. In the preparation process, the weight ratio of BFS/HL is the most important preparation variable for P adsorption capacity and excess improvement. Furthermore, it was found that the adsorption model of phosphate onto sorbents was consistent with Langmuir model, and the adsorption process could be described by the pseudo-second-order model. This article gave a promising result for applying the BFS–HL sorbent in P adsorption from aqueous solution, and the further investigation with real wastewater will be conducted in our lab for utilization of the waste resource of BFS.

Acknowledgement

This work was supported by National Science Foundation of China (No. 50774073).

References

[1] H. Yamada, M. Kayama, K. Saito, M. Hara, A fundamental research on phosphate removal by using slag, Water Res. 20 (1986) 547–557.
[2] D.C. Southam, T.W. Lewis, A.J. McFarlane, J.H. Johnston, Amorphous calcium silicate as a chemisorbent for phosphate, Curr. Appl. Phys. 4 (2004) 355–358.
[3] M. Khadhraoui, T. Watanabe, M. Kuroda, The effect of the physical structure of a porous Ca-based sorbent on its phosphorus removal capacity, Water Res. 36 (2002) 3711–3718.
[4] B. Kostura, H. Kulveitová, J. Leško, Blast furnace slags as sorbents of phosphate from water solutions, Water Res. 39 (2005) 1795–1802.
[5] N.M. Agyei, C.A. Strydom, J.H. Potgieter, The removal of phosphate ions from aqueous solution by fly ash, slag, ordinary Portland cement and related blends, Cem. Concr. Res. 32 (2002) 1889–1897.
[6] M. Özacar, Equilibrium and kinetic modelling of adsorption of phosphorus on calcined alunite, Adsorption 9 (2003) 125–132.
[7] E.C. Ou, J.J. Zhou, S.C. Mao, J.Q. Wang, F. Xia, L. Min, Highly efficient removal of phosphate by lanthanum-doped mesoporous SiO_2, Colloids Surf. 308 (2007) 47–53.
[8] A. Genz, A. Kornmuller, M. Jekel, Advanced phosphorus removal from membrane filtrates by adsorption on activated aluminium oxide and granulated ferric hydroxide, Water Res. 38 (2004) 3523–3530.
[9] A.L. Gimsing, C. Szilas, O.K. Borggaard, Sorption of glyphosate and phosphate by variable-charge tropical soils from Tanzania, Geoderma 138 (2007) 127–132.
[10] J.G. Chen, H.N. Kong, D.Y. Wu, X.C. Chen, D.L. Zhang, Z.H. Sun, Phosphate immobilization from aqueous solution by fly ashes in relation to their composition, J. Hazard. Mater. B 139 (2007) 293–300.
[11] K.C. Cheung, T.H. Venkitachalam, Improving phosphate removal of sand infiltration system using alkaline fly ash, Chemosphere 41 (2000) 243–249.
[12] Y.Z. Li, C.J. Liu, Z.K. Luan, X.J. Peng, C.L. Zhu, Z.Y. Chen, Z.G. Zhang, J.H. Fan, Z.P. Jia, Phosphate removal from aqueous solutions using raw and activated red mud and fly ash, J. Hazard. Mater. B137 (2006) 374–383.
[13] M.Y. Can, E. Yildiz, Phosphate removal from water by fly ash—factorial experimental design, J. Hazard. Mater. B 135 (2006) 165–170.
[14] L. Johansson, J.P. Gustafsson, Phosphate removal using blast furnace slags and opoka-mechanisms, Water Res. 34 (2000) 259–265.
[15] Y.H. Moon, J.G. Kim, J.S. Ahn, G.H. Lee, H.S. Moon, Phosphate removal using sludge from fuller's earth production, J. Hazard. Mater. 143 (2007) 41–48.
[16] L.D. Hylander, A. Kietlińska, G. Renman, G. Simán, Phosphorus retention in filter materials for wastewater treatment and its subsequent suitability for plant production, Bioresour. Technol. 97 (2006) 914–921.
[17] J.G. Chen, H.N. Kong, D.Y. Wu, Z.B. Hu, Z.S. Wang, Y.H. Wang, Removal of phosphate from aqueous solution by zeolite synthesized from fly ash, J. Colloid Interface Sci. 300 (2006) 491–497.
[18] L.E. de-Bashan, Y. Bashan, Recent advances in removing phosphorus from wastewater and its future use as fertilizer (1997–2003), Water Res. 38 (2004) 4222–4246.
[19] E.H. Kim, D.W. Lee, H.K. Hwang, S. Yim, Recovery of phosphates from wastewater using converter slag Kinetics analysis of a completely mixed phosphorus crystallization process, Chemosphere 63 (2006) 192–201.
[20] G.G. Jayson, T.A. Lawless, D. Fairhurst, The adsorption of organic and inorganic phosphates onto a new activated carbon adsorbent, J. Colloid Interface Sci. 86 (1982) 397–410.
[21] M.A. Ferro-Garca, F. Carrasco-Marn, J. Rivera-Utrilla, E. Utrera-Hidalgo, C. Moreno-Castilla, The use of activated carbon columns for the removal of orthophosphate ions from aqueous solutions, Carbon 28 (1990) 91–95.
[22] E. Oguz, Removal of phosphate from aqueous solution with blast furnace slag, J. Hazard. Mater. B 114 (2004) 131–137.
[23] R.B. Lin, S.M. Shih, C.F. Liu, Structural properties and reactivities of $Ca(OH)_2$/fly ash sorbents for flue gas desulfurization, Ind. Eng. Chem. Res. 42 (2003) 1350–1356.
[24] J. Fernamdez, M.J. Renedo, A. Pesquera, J.A. Irabien, Effect of $CaSO_4$ on the structure and use of $Ca(OH)_2$/fly ash sorbents for SO_2 removal, Powder Technol. 119 (2001) 201–205.
[25] H.F.W. Taylor, Chemistry of Cement, Academic Press, Harcourt Brace Jovanovich Publishers, London, 1990.
[26] R.B. Lin, S.M. Shih, Characterization of $Ca(OH)_2$/fly ash sorbents for flue gas desulfurization, Powder Technol. 131 (2003) 212–222.
[27] T. Ishizuka, T. Yamamoto, T. Murayama, T. Tanaka, H. Hattori, Effect of calcium sulfate addition on the activity of the absorbent for dry flue gas desulfurization, Energy Fuels 15 (2001) 438–443.
[28] B.K. Biswas, K. Inoue, K.N. Ghimire, S. Ohta, H. Harada, K. Ohto, H. Kawakita, The adsorption of phosphate from an aquatic environment using metal-loaded orange waste, J. Colloid Interface Sci. 312 (2007) 214–223.